

# InternLM-XComposer: A Vision-Language Large Model for Advanced Text-image Comprehension and Composition

Pan Zhang<sup>\*1</sup>, Xiaoyi Dong<sup>\*1</sup>, Bin Wang<sup>1</sup>, Yuhang Cao<sup>1</sup>, Chao Xu<sup>1</sup>, Linke Ouyang<sup>1</sup>, Zhiyuan Zhao<sup>1</sup>, Shuangrui Ding<sup>1</sup>, Songyang Zhang<sup>1</sup>, Haodong Duan<sup>1</sup>, Hang Yan<sup>1</sup>, Xinyue Zhang<sup>1</sup>, Wei Li<sup>1</sup>, Jingwen Li<sup>1</sup>, Kai Chen<sup>1</sup>, Conghui He<sup>1</sup>, Xingcheng Zhang<sup>1</sup>, Yu Qiao<sup>1</sup>, Dahua Lin<sup>1</sup>, Jiaqi Wang<sup>1,✉</sup>

<sup>1</sup>Shanghai Artificial Intelligence Laboratory

internlm@pjlab.org.cn

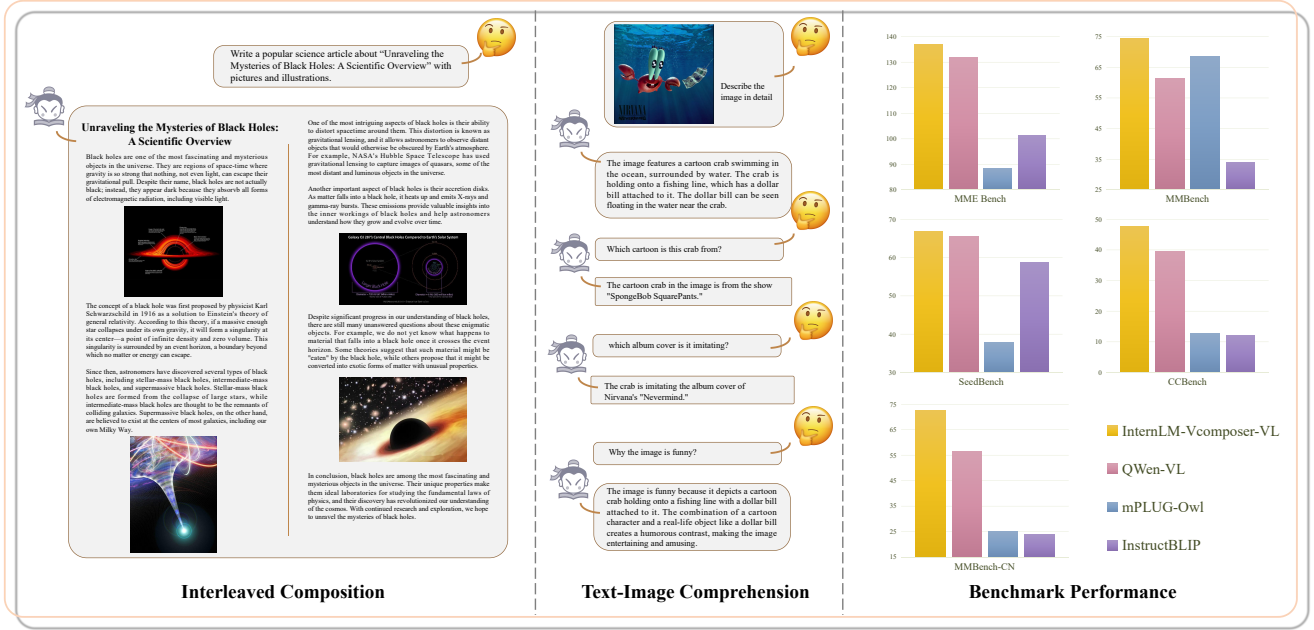


Figure 1. The InternLM-XComposer shows excellent interleaved composition and text-image comprehension ability, leading to strong performance on various multimodal benchmarks.

## Abstract

We propose *InternLM-XComposer*, a vision-language large model that enables advanced image-text comprehension and composition. The innovative nature of our model is highlighted by three appealing properties: 1) **Interleaved Text-Image Composition**: *InternLM-XComposer* can effortlessly generate coherent and contextual articles that seamlessly integrate images, providing a more engaging and immersive reading experience. Simply provide a title, and our system will generate the corresponding manuscript. It can intelligently identify the areas in the text where images would enhance the content and automatically insert the most appropriate visual candidates. 2) **Comprehension**

**with Rich Multilingual Knowledge**: The text-image comprehension is empowered by training on extensive multimodal multilingual concepts with carefully crafted strategies, resulting in a deep understanding of visual content. 3) **State-of-the-art Performance**: Our model consistently achieves state-of-the-art results across various mainstream benchmarks for vision-language foundational models, including MME Benchmark, MMBench, MMBench-CN, Seed-Bench, and CCBench (Chinese Cultural Benchmark). Collectively, *InternLM-XComposer* seamlessly blends advanced text-image comprehension and composition, revolutionizing vision-language interaction and offering new insights and opportunities. The *InternLM-XComposer* models with 7B parameters are publicly available at <https://github.com/InternLM/InternLM-XComposer>.

\* indicates equal contribution.

## 1. Introduction

Over the past year, impressive progress has been made in developing large language models (LLMs) [4, 5, 9, 10, 16, 46, 47, 51, 54, 62–64]. These state-of-the-art models, including ChatGPT [46], GPT4 [47], and PaLM 2 [10], have shown an unprecedented ability to follow human instructions and solve open-ended tasks. Inspired by the success of PaLM-E [15] and BLIP2 [31], there is a promising approach to extending language models for vision-language tasks by leveraging vision features as extra inputs of LLMs. The community has developed several vision-language large models (VLLMs), such as MiniGPT-4 [79], LLaVA [38], and InstructBLIP [11], based on open-source LLMs like LLaMA [63], GLM [16], and InternLM [62]. However, these VLLMs focus on pure text outputs, missing the opportunity to equip generated text with richer information through auxiliary multimedia content like images.

In this work, we propose InternLM-XComposer, which is a vision-language large model that enables advanced text-image comprehension and composition ability.

1) **Interleaved Text-Image Composition.** InternLM-XComposer excels in generating long-form content that is interleaved with contextually relevant images, thereby elevating the experience of vision-language interaction. In its operational flow, the framework first crafts text based on human-provided instructions. Subsequently, it autonomously pinpoints optimal locations within the text for image placement and furnishes corresponding, suitable image descriptions. In accordance with the generated descriptions, instead of relying on a text-image generation model for assistance, we opt to source aligned images from a large-scale web-crawled image database for realistic quality and contextual alignment. Moreover, it also provides flexibility by allowing users to customize an image repository.

Compared to a baseline approach that relies solely on CLIP [52, 68] for image retrieval, XComposer offers a more reliable solution for choosing the most appropriate image. Initially, we select potential image candidates from our database using CLIP. Then, InternLM-XComposer leverages its comprehension capabilities to identify the image that optimally complements the content.

2) **Comprehension with Rich Multilingual Knowledge.** LLM demonstrates remarkable generalizability in handling open-world tasks, a capability attributed to its extensive training data, *e.g.*, 2T tokens used in LLaMA2 [64]. This vast dataset inherently encapsulates a broad spectrum of semantic knowledge across diverse domains. In contrast, existing vision-language datasets are relatively constrained in both volume and diversity. To tackle these limitations, we employ two practical solutions: First, an interleaved multilingual vision-language dataset with over 11 million semantic concepts is collected from public websites. Second, we carefully crave the pretraining and finetuning strategies in

our training pipeline, where we adopt the mixed training data of pure text and image-text data, primarily in English and Chinese. Consequently, InternLM-XComposer demonstrates a remarkable proficiency in comprehending a wide array of image content and responding with an extensive repository of multilingual knowledge.

The proposed InternLM-XComposer exhibits superior capabilities in both text-image comprehension and composition, as evidenced by its strong performance in quantitative benchmarks and compelling qualitative demonstrations. It consistently achieves **state-of-the-art** performance across various leading benchmarks for vision-language large models, encompassing MME Benchmark [18, 71], MMBench [72], Seed-Bench [29] in English, and MMBench-CN [72], CCBench (Chinese Cultural Benchmark) [72] for evaluations in Chinese. Notably, our method significantly outperforms existing frameworks on benchmarks in the Chinese language, *i.e.*, MMBench-CN [72] and CCBench [72], demonstrating unparalleled multilingual knowledgeability.

We release InternLM-XComposer series in two versions:

- InternLM-XComposer-VL: The pretrained VLLM model with InternLM [62] as the initial LLM.
- InternLM-XComposer: The supervised finetuned VLLM for interleaved text-image composition and LLM-based AI assistant.

## 2. Related Works

**Large Language Models.** In recent years, the development of large language models has accelerated. Initially, encoder-decoder models such as BERT [14] and T5 [54], as well as decoder-only models like GPT [53], leveraged the Transformer architecture [65] to achieve remarkable results across various NLP tasks. GPT3 [5], employing prompt and in-context learning strategies along with larger models and data, has shown significant performance in few-shot and zero-shot downstream tasks. As a result, using decoder-only structures based on autoregressive decoding for output prediction has gained popularity among researchers. Google’s PaLM [10] further expands the model parameter size and data volume, setting the performance benchmark of the time. To enhance the practical conversational experience, models like InstructGPT [49] and ChatGPT [46] integrate fine-tuning and reinforcement learning strategies guided by human feedback to guide models toward human-like conversation. The open-sourcing of the LLaMA [63] model has invigorated research on large language models, leading to the successive open-sourcing of a series of notable large language models such as Vicuna [9], Qwen [51], LLaMA2 [64], Baichuan2 [4], and InternLM [62].

**Multimodal Large Language Models.** Like large language models, visual language learning has emerged as a

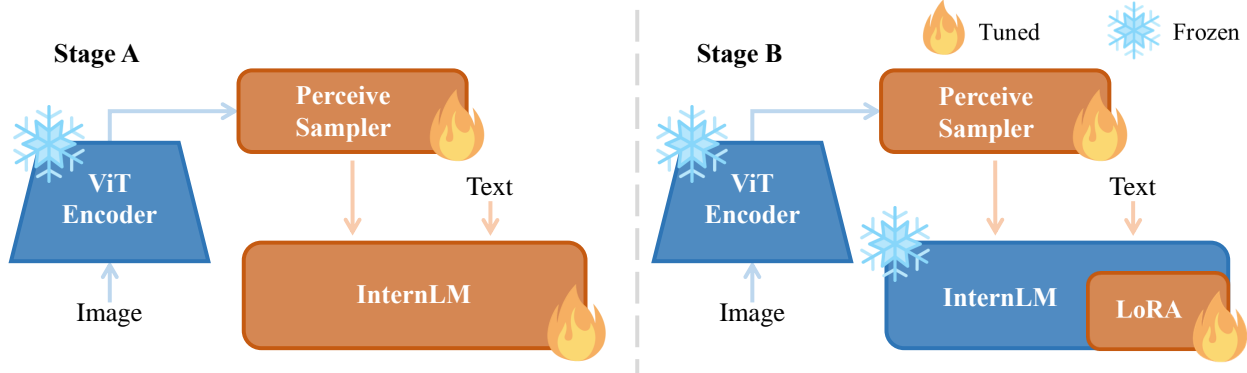


Figure 2. **The architecture of the InternLM-XComposer.** The proposed model comprises three essential components: a visual encoder, a perceive sampler, and a large language model. The training regimen is divided into two distinct phases, namely Stage A and Stage B. In Stage A, which serves as the pre-training phase, both the perceive sampler and the large language model are subjected to optimization procedures. Stage B focuses on supervised fine-tuning, during which the perceive sampler and LoRA [23] are specifically trained.

research hotspot in computer vision. Initially, these models utilized the Transformer architecture to align image-text pairs in unsupervised samples, enabling strong performance in zero-shot learning tasks like Image Captioning and Image-Text Retrieval. CLIP [52] aligns image and text features through contrastive learning objectives on large-scale image-text pairs, outperforming supervised learning on ImageNet [13] and exhibiting strong generalization capabilities in various downstream tasks. BLIP [32] devises data selection and generation strategies using cleaner and more diversified data, outperforming CLIP. Information mined from image-text pairs can effectively provide labels for basic visual tasks [34, 39, 74]. However, these models show limited capabilities for tasks requiring higher-level understanding, such as visual question answering. Benefiting from existing large language model [9] and visual encoder [17], MiniGPT-4 [79] trains multimodal large language models (MLLMs) through pre-training feature alignment and instruction fine-tuning, exhibiting excellent image-text dialogue capabilities. For the instruction fine-tuning stage of MLLMs, a series of studies [38, 66, 78] have explored the impact of the quality, diversity, and specificity of the fine-tuning data on the performance of these models, further enhancing their performance. MMICL [76] can manage multiple image inputs, enabling multimodal models to understand more complex Prompts. Otter [30], built on the OpenFlamingo [2] structure and multimodal context instruction fine-tuning data, can better follow new instructions. InstructBLIP [11], based on various image-text datasets, fine-tunes MLLMs by constructing prompt templates and introduces Q-Former [32] to associate more relevant image features in advance. With a larger dataset, this model shows better generalization capabilities across multiple tasks. mPLUG-Owl [70] introduces additional text-only instruction data during the second phase of in-

struction fine-tuning, improving its capabilities. Shikra [7] and KOSMOS-2 [50] incorporate Grounding data during the training phase, enabling the model to develop Grounding capabilities, reduce hallucinations, and enhance performance. Qwen-VL [3] uses more pre-training data and higher-resolution inputs to deepen the model’s understanding of image-text details.

**Multimodal Retrieval Models.** Image-text retrieval, a pivotal area in multimodal modeling, has seen substantial advancements recently. CLIP [52], utilizing contrastive learning on a large corpus of unsupervised image-text pairs, excels in image-text matching, enabling efficient retrieval in both image-to-text and text-to-image modalities. Expanding on CLIP’s foundation, BLIP [32] filters out irrelevant image-text pairs, generating a high-quality subset for retraining, thereby enhancing image-text matching performance. ALIGN [27] extends beyond singular image-text matching by simultaneously accommodating image-text combinations as inputs, retrieving results that meet the given image-text criteria, thus providing a more comprehensive retrieval system. Despite these models’ impressive strides in image-text retrieval, they still need to improve in deep image-text understanding. REVEAL [25] addresses this by introducing an end-to-end retrieval-enhanced visual language model that leverages various knowledge source modalities and operates in tandem with a generator, excelling in knowledge-intensive visual question-answering tasks. RA-CM3 [69] further enhances this process by retrieving external relevant knowledge as a supplement, facilitating superior generation of image and text results, and demonstrating remarkable performance in knowledge-intensive image generation and multimodal in-context learning tasks. FROMAGE [28] integrates the large language model [75] with the visual encoder CLIP ViT/14 [52]. Training with image-text pairs utilizes multi-

modal information from multi-turn dialogues for image retrieval and conversation, offering a more dynamic and interactive approach to retrieval. However, the capabilities of current models are primarily confined to the matching and generation of image-text pairs, revealing a significant gap in their ability to generate comprehensive interleaved image-text articles, signifying a promising future research direction.

### 3. Method

#### 3.1. Model Architecture

In the proposed InternLM-XComposer framework, as depicted in Figure 2, there are three integral components: a visual encoder, a perceive sampler, and a large language model.

**Visual Encoder.** The visual encoder in InternLM-XComposer employs EVA-CLIP [17], an refined variant of the standard CLIP [68], enhanced with mask image modeling capabilities, to proficiently capture the visual nuances of the input image. Within this module, images are resized to a consistent dimension of  $224 \times 224$  and subsequently dissected into patches with a stride of 14. These patches serve as input tokens and enable the self-attention mechanisms within the transformer block, facilitating the extraction of detailed image embeddings.

**Perceive Sampler.** The perceive sampler within the InternLM-XComposer operates as an attentive pooling mechanism designed to condense the initial set of 257 image embeddings down to 64 refined embeddings. These optimized embeddings are subsequently aligned to be compatible with the knowledge structures understood by the large language model. Following BLIP2 [31], we leverage BERT<sub>base</sub> [14] equipped with cross-attention layers, serving as the perceive sampler in our framework.

**Large Language Model.** The InternLM-XComposer is anchored on InternLM [62] as its foundational large language model. Notably, InternLM stands as a potent language model equipped with bilingual capabilities, proficient in both English and Chinese. In our framework, we employ the publicly available InternLM-7B and InternLM-20B to serve as the large language models. For comprehensive details about InternLM, we refer readers to its official code repository<sup>1</sup>.

#### 3.2. Training

As shown in Figure 2, the training process of InternLM-XComposer is split into Stage A and Stage B. Stage A serves as the pre-training phase, utilizing vast amounts of data for foundational model training. In contrast, Stage B functions as a supervised fine-tuning phase, drawing on

a select dataset of high precision to enhance the model’s instruction-following capabilities.

**Pre-training.** The pre-training phase incorporates large-scale, web-crawled image-text pairs along with interleaved image-text data to pre-train the foundational vision-language model. This data comprises multimodal content in both English and Chinese languages. To preserve the linguistic capabilities of the large language model, the partial textual data utilized for InternLM’s pre-training is also employed in the pre-training phase of InternLM-XComposer. As indicated in Table 1, the multimodal pre-training process employs 1.1 billion images alongside 67.7 billion text tokens, including both public datasets and in-house data collected from public websites, possessing over 11 million semantic concepts. This corpus includes 50.6 billion English text tokens and 17.1 billion Chinese text tokens. Furthermore, approximately 10 billion text tokens, sampled from the InternLM pre-training dataset, are incorporated to maintain the model’s linguistic proficiencies. Prior to the training process, all pre-training data underwent a thorough cleaning procedure to ensure its quality and reliability.

During the pre-training phase, the visual encoder is held constant, allowing for the optimization to be concentrated on the perceive sampler and the large language model. Initial weight for the perceive sampler and the large language model are sourced from BLIP2 [31] and InternLM [62], respectively. Given that the large language model lacks native understanding of image embeddings, its optimization within the framework of multimodal pre-training serves to enhance its capability to interpret such embeddings effectively. The training objective for the model centers on next-token prediction, utilizing cross-entropy loss as the loss function. The optimization algorithm employed is AdamW, with hyperparameter settings as follows:  $\beta_1=0.9$ ,  $\beta_2=0.95$ ,  $\epsilon=1e-8$ . The maximum learning rates for the perceive sampler and the large language model are configured at  $2e-4$  and  $4e-5$ , respectively, following a cosine learning rate schedule. The minimum learning rate is set at  $1e-5$ . Additionally, a linear warm-up is applied over the initial 200 steps. The training procedure employs a batch size of approximately 15.7 million tokens and spans 8,000 iterations. Utilizing such a large batch size in conjunction with a limited number of iterations contributes to stable training dynamics while also aiding in the preservation of the inherent capabilities of InternLM.

**Supervised Fine-Tuning.** In the pre-training phase, image embeddings are aligned with language representations, equipping the large language model with a rudimentary understanding of image content. However, the model still lacks proficiency in utilizing this image information optimally. To address this limitation, we introduce a variety of vision-language tasks that the model undertakes during the subsequent Supervised Fine-Tuning Stage (SFT).

<sup>1</sup><https://github.com/InternLM/InternLM>

Language	Type	Dataset	Selected Images	Selected Text
English	Image-text paired	SBU-Caption [48])	1M	18M
	Image-text paired	Conceptual Captions 3M [58]	3M	37M
	Image-text paired	Conceptual 12M [6]	9M	250M
	Image-text paired	LAION400M [56]	509M	10B
	Image-text paired	In-house Data	2M	321M
	Interleaved image-text	Multimodal C4 [80]	332M	40B
Chinese	Image-text paired	WuKong [21]	31M	545M
	Image-text paired	TaiSu [40]	44M	865M
	Image-text paired	LAION-CN [55]	80M	2B
	Image-text paired	In-house Data	9M	704M
	Interleaved image-text	In-house Data	85M	13B
Total			1.1B	67.7B

Table 1. Details of InternLM-XComposer pre-training multimodal data. LAION-CN represents the Chinese language subset extracted from the larger LAION-5B corpus. This subset is further cleaned utilizing the Chinese CLIP [68]. The volume of text data is counted in terms of the number of tokens. The in-house data are collected from public websites, possessing over 11 million semantic concepts collected from public websites. A subset of the in-house data has been made publicly available by WanJuan [22].

Task	Dataset
<i>Multi-task training</i>	
Caption	COCO [8], SUB [8], TextCaps [59]
VQA	VQAv2 [1], GQA [26], OK-VQA [44], VSR [35], IConQA [42] Text-VQA [60], SQA [41], OCR-VQA [45], In-house data
IQG	VQAv2 [1], OK-VQA [44], A-OKVQA [57]
Conversation	Visual Dialog [12], LLaVA-150k [38]
<i>Instruction tuning</i>	
Image-Text Composition	In-house data (Refer to Sec.3.3)
Conversation	LLaVA-150k [38], Alpaca-en&zh [61], ShareGPT-en&zh, Oasst-en&zh, LRV [36]

Table 2. Datasets used for Supervised Fine-Tuning.

As illustrated in Table 2, the SFT dataset is constructed from multiple sources to endow the model with a diverse range of capabilities. These include scene understanding (e.g., COCO Caption [8], SUB [48]), location understanding (e.g., Visual Spatial Reasoning dataset [35]), Optical Character Recognition (OCR) (e.g., OCR-VQA [45]), and open-ended answering (e.g., VQAv2 [1], GQA [26]), among others. Each of these tasks is formulated as a conversational interaction, adhering to the following format:

$\langle |User| \rangle$ : *Instruction*  $\langle eou \rangle$   
 $\langle |Bot| \rangle$ : *Answer*  $\langle eob \rangle$

where  $\langle eou \rangle$  and  $\langle eob \rangle$  represent the *end-of-user* and *end-of-bot* tokens, respectively. For QVA datasets featuring multiple questions per image, we structure them as multi-round conversations with randomly ordered questions, thereby substantially enhancing the efficiency of the

SFT process. During this stage, all questions are introduced through manually crafted prompts to augment task diversity.

In order to achieve stable and efficient fine-tuning, we retain the weights of the pre-existing large language model in a frozen state. Subsequently, we augment the architecture with Low-Rank Adaption (LoRA) [23] for the fine-tuning process. The perceive sampler is concurrently trained, albeit with a distinct learning rate. Specifically, LoRA is applied to the *query*, *value* and *key* of the attention layer as well as the feed-forward network. We find that a high LoRA rank is conducive for imbuing the model with new capabilities; consequently, we set the LoRA rank and alpha parameter both to 256. The model is trained using a global batch size of 256 over 10,000 iterations. The learning rates are set to  $5e^{-5}$  for the LoRA layer and  $2e^{-5}$  for the perceive sampler.

To further empower aforementioned model’s instruction following and interleaved image-text composition capabil-

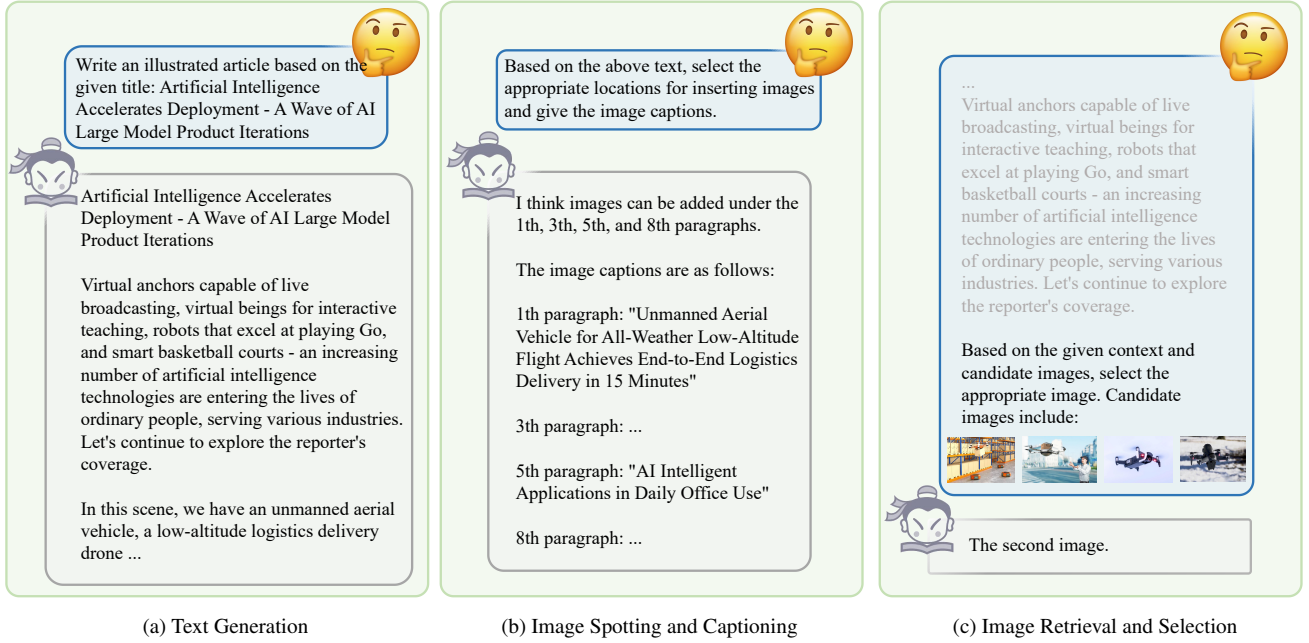


Figure 3. **The pipeline of the interleaved image-text composition.** (a) Given an input title, the model initially generates a corresponding text-based article. (b) Subsequent to the article generation, the model is trained to identify suitable image locations and generate corresponding captions for the ensuing steps. (c) A text-image retrieval algorithm is initially employed to constrict the pool of candidate images. Following this, our vision-language model is fine-tuned to make the final image selection, ensuring thematic and visual coherence by considering both the preceding textual content and images within the article.

ity, we utilize data from pure-text conversation corpora and LLaVA-150k for instruction-based tuning, and leverage the LRV dataset to mitigate hallucinations. The interleaved image-text composition dataset is constructed based on the methodology delineated in Section 3.3. We maintain a batch size of 256 and execute the tuning over 1000 iterations with a small learning rate  $1e^{-5}$ .

### 3.3. Interleaved Image-Text Composition

To achieve the objective of crafting interleaved image-text compositions, the initial step involves the generation of a text-centric article. Following this, pertinent images are incorporated at well-suited positions within the textual content, thereby enriching the overall narrative and augmenting reader engagement.

**Text Generation.** To facilitate the generation of extended text-based articles, we curate a dataset comprising interleaved image-text compositions. It is noteworthy that the acquired dataset contains noise, particularly in the form of marketing and advertising content. To address this, we employ GPT-4 to assess the noise level of each individual paragraph. Any paragraphs that are identified as noisy, along with articles where over 30% of the content is classified as such, are subsequently filtered out of the dataset.

To enable the model to generate text-based articles with

respect to specific titles, we formulate the training data in the following manner:

$\langle |User| \rangle$ : Write an illustrated article based on the given title:  $\{Title\}$   $\langle eou \rangle$   
 $\langle |Bot| \rangle$ :  $[para_1] \dots [para_N]$   $\langle eob \rangle$

Here,  $\{Title\}$  serves as a placeholder for the article title, while  $[para_1]$  and  $[para_N]$  denote the first and last paragraphs, respectively.

To enhance the visual appeal and engagement level of the generated text-centric articles, the incorporation of contextually appropriate images is essential. In line with this aim, we establish an exhaustive database that functions as a candidate pool for the selection of images. The overall procedure is divided into two main components: image spotting, which identifies opportune locations within the text for image integration, and image selection, aimed at choosing the most contextually suitable images.

A basic strategy for image selection involves summarizing the preceding textual content and retrieving the most closely related image from the available image pool. However, this approach is insufficient for maintaining a coherent thematic flow of images across the article. To remedy this limitation, we suggest the employment of our vision-

Model	Overall	Exist.	Count	Pos.	Color	OCR	Poster	Cele.	Scene	Land.	Art.	Comm.	NumCal.	Trans.	Code	Avg.
LLaVA [38]	712.5	50.0	50.0	50.0	50.0	50.0	50.0	48.8	50.0	50.0	49.0	57.1	50.0	57.5	50.0	50.9
MiniGPT-4 [79]	694.3	68.3	55.0	43.3	43.3	57.5	41.8	54.4	71.8	54.0	60.5	59.3	45.0	0.0	40.0	49.6
MM-GPT [20]	871.5	61.7	55.0	58.3	58.3	82.5	57.8	73.8	68.0	69.8	59.5	49.3	62.5	60.0	55.0	62.3
VisualGLM [16]	880.4	85.0	50.0	48.3	48.3	42.5	66.0	53.2	146.3	83.8	75.3	39.3	45.0	50.0	47.5	62.9
LaVIN [43]	1201.6	185.0	88.3	63.3	63.3	107.5	79.6	47.4	136.8	93.5	87.3	87.1	65.0	47.5	50.0	85.8
mPLUG-Owl [70]	1238.4	120.0	50.0	50.0	50.0	65.0	136.1	100.3	135.5	159.3	96.3	78.6	60.0	80.0	57.5	88.5
LLaMA-A.-V2 [19]	1194.9	120.0	50.0	48.3	48.3	<u>125.0</u>	99.7	86.2	148.5	150.3	69.8	81.4	62.5	50.0	55.0	85.4
InstructBLIP [11]	1417.9	185.0	143.3	66.7	66.7	72.5	123.8	101.2	153.0	79.8	134.3	129.3	40.0	65.0	57.5	101.3
BLIP-2 [31]	1508.8	160.0	135.0	73.3	73.3	110.0	141.8	105.6	145.3	138.0	136.5	110.0	40.0	65.0	75.0	107.8
Lynx [73]	1508.9	<u>195.0</u>	<u>151.7</u>	90.0	90.0	77.5	124.8	118.2	<u>164.5</u>	<u>162.0</u>	119.5	110.7	17.5	42.5	45.0	107.8
GIT2 [67]	1532.2	<u>190.0</u>	118.3	<u>96.7</u>	96.7	65.0	112.6	145.9	158.5	140.5	<u>146.3</u>	99.3	50.0	67.5	45.0	109.4
LRV-Instruct [37]	1549.7	165.0	111.7	86.7	86.7	110.0	139.0	112.7	148.0	160.5	101.3	100.7	70.0	85.0	72.5	110.7
Otter [30]	1572.0	<u>195.0</u>	88.33	86.7	86.7	72.5	138.8	<u>172.7</u>	<u>158.8</u>	137.3	129.0	106.4	<u>72.5</u>	57.5	70.0	112.3
Cheetor [33]	1584.4	180.0	96.7	80.0	80.0	100.0	147.3	<u>164.1</u>	156.0	145.7	113.5	98.6	<u>77.5</u>	57.5	<u>87.5</u>	113.2
BLIVA [24]	1669.2	180.0	138.3	81.7	<u>180.0</u>	87.5	<u>155.1</u>	140.9	151.5	89.5	<u>133.3</u>	<u>136.4</u>	57.5	77.5	60.0	119.2
MMICL [77]	1810.7	170.0	<u>160</u>	81.7	156.7	100	146.3	141.8	153.8	136.13	<u>135.5</u>	<u>136.4</u>	<u>82.5</u>	<u>132.5</u>	<u>77.5</u>	129.3
Qwen-VL-Chat [3]	1848.3	158.3	150.0	<u>128.3</u>	<u>170.0</u>	<u>140.0</u>	<u>178.6</u>	120.6	152.3	<u>164.0</u>	125.5	130.7	40.0	<u>147.5</u>	42.5	132.0
Ours	1919.5	<u>190.0</u>	<u>158.3</u>	<u>126.7</u>	<u>165.0</u>	<u>125.0</u>	<u>161.9</u>	<u>150.3</u>	<u>159.8</u>	<u>165.3</u>	126.3	<u>138.6</u>	55.0	<u>112.5</u>	<u>85.0</u>	<b>137.1</b>

Table 3. **Evaluation of MME-Benchmark.** Here we report the results on all the sub tasks, including Existence(Exist.), Count, Position(Pos.), Color, OCR, Poster, Celebrity(Cele.), Scene, Landmark(Land.), Artwork(Art.), Commonsense Reasoning(Comm.), Numerical Calculation(NumCal.), Text Translation(Trans.), Code Reasoning(Code) and the task-level average (Avg.). We **bold** the highest average score and highlight the Top-3 model of each sub task with underline.

Method	Language Model	Vision Model	Overall	LR	AR	RR	FP-S	FP-C	CP
MMGPT	LLaMA-7B	CLIP ViT-L/14	16.0	1.1	23.8	20.7	18.3	5.2	18.3
MiniGPT-4	Vincuna-7B	EVA-G	23.0	13.6	32.9	8.9	28.8	11.2	28.3
PandaGPT	Vincuna-13B	ImageBind ViT-H/14	30.6	15.3	41.5	22.0	20.3	20.4	47.9
VisualGLM	ChatGLM-6B	EVA-CLIP	33.5	11.4	48.8	27.7	35.8	17.6	41.5
InstructBLIP	Vincuna-7B	EVA-G	33.9	21.6	47.4	22.5	33.0	24.4	41.1
LLaVA	LLaMA-7B	CLIP ViT-L/14	36.2	15.9	53.6	28.6	41.8	20.0	40.4
LLaMA-Adapter-v2	LLaMA-7B	CLIP ViT-L/14	38.9	7.4	45.3	19.2	45.0	32.0	54.0
G2PT	LLaMA-7B	ViT-G	39.8	14.8	46.7	31.5	41.8	34.4	49.8
Otter-I	LLaMA-7B	CLIP ViT-L/14	48.3	22.2	63.3	39.4	46.8	36.4	60.6
IDEFICS-80B	LLaMA65B	CLIP ViT-H/14	54.6	29.0	67.8	46.5	56.0	48.0	61.9
Shikra	Vincuna-7B	CLIP ViT-L/14	60.2	33.5	69.6	53.1	61.8	50.4	71.7
Qwen-VL-Chat	Qwen-7B	ViT-G/16	61.2	38.6	70.9	46.9	67.7	47.6	71.9
LMEye	Flan-XL	CLIP ViT-L/14	61.3	36.9	73.0	55.4	60.0	58.0	68.9
MMICL	FLANT5-XXL	EVA-G	65.2	44.3	77.9	64.8	66.5	53.6	70.6
mPLUG-Owl	LLaMA2-7B	CLIP ViT-L/14	68.5	<b>56.8</b>	77.9	62.0	72.0	58.4	72.6
InternLM-XComposer-VL	InternLM	EVA-G	<b>74.4</b>	50.6	<b>82.0</b>	<b>76.1</b>	<b>79.3</b>	<b>59.2</b>	<b>81.7</b>

Table 4. **Evaluation of MMBench test set.** Here we report the results on the six L-2 abilities, namely Logical Reasoning (LR), Attribute Reasoning (AR), Relation Reasoning (RR), Fine-grained Perception (Cross Instance) (FP-C), Fine-grained Perception (Single Instance) (FP-S), and Coarse Perception (CP).

language foundational model. This model is designed to select a portfolio of images that are not only contextually relevant but also maintain thematic consistency throughout the article.

In order to enhance computational efficiency, we initially employ a retrieval mechanism to reduce the size of the candidate image pool. Subsequent to this, our vision-language model is deployed to perform the final image selection from this narrowed set of candidates. Consequently, the overar-

ching task is decomposed into image spotting and captioning, along with image retrieval and selection.

**Image Spotting and Captioning.** Leveraging the acquired interleaved image-text compositions, pinpointing image locations becomes a straightforward task. For subsequent image retrieval, it’s imperative to generate an appropriate caption, enabling the application of various text-image retrieval algorithms. A straightforward approach involves employing a large language model to summarize preceding content as

Method	Language Model	Overall	T-Avg.	Sense.U	Inst.Id	Inst.At	Inst.Lo	Inst.Co	Spat.R	Inst.It	Vis.R	Text.R
OpenFlamingo	MPT-7B	42.7	39.4	53.2	45.3	40	31.2	39.3	32.6	36.1	51.4	25.9
Otter	MPT-7B	42.9	40.08	51.3	43.5	42.3	34.2	38.4	30.9	40.2	55.3	24.7
IDEFICS-9b-instruct	LLaMA-7B	44.5	43.01	55.8	45.3	42.3	40.2	36.8	34.9	37.1	55.9	38.8
MiniGPT-4	Vicuna-7B	47.4	42.6	56.3	49.2	45.8	37.9	45.3	32.6	47.4	57.1	11.8
BLIP-2	Flan-T5-XL	49.7	45.7	59.1	53.9	49.2	42.3	43.2	36.7	55.7	45.6	25.9
IDEFICS-80b-instruct	LLaMA-65B	53.2	54.4	64	52.6	50.8	48.3	46.1	45.5	62.9	68	51.8
Kosmos-2	Kosmos 1.3B	54.4	49.4	63.4	57.1	58.5	44	41.4	37.9	55.7	60.7	25.9
InstructBLIP	Flan-T5-XL	57.8	49.3	60.3	58.5	63.4	40.6	<b>58.4</b>	38.7	51.6	45.9	25.9
InstructBLIP-Vicuna	Vicuna-7B	58.8	52.2	60.2	58.9	65.6	43.6	57.2	40.3	52.6	47.7	43.5
Qwen-VL	Qwen-7B	62.3	59.6	71.2	66.4	67.7	53.5	44.8	43.8	62.9	74.9	51.2
Qwen-VL-Chat	Qwen-7B	65.4	61.9	73.3	67.3	<b>69.6</b>	57.7	52.9	48.2	59.8	74.6	<b>53.5</b>
InternLM-XComposer-VL	InternLM-7B	<b>66.9</b>	<b>65.2</b>	<b>75.0</b>	<b>71.7</b>	67.6	<b>60.8</b>	56.2	<b>55.3</b>	<b>74.4</b>	<b>77.0</b>	48.5

Table 5. **Evaluation of Seed-Bench test set.** Here we report the results on the image-based sub tasks, including Scene Understanding(Sense.U), Instance Identity(Inst.Id), Instance Attributes(Inst.At), Instance Localization(Inst.Lo), Instance Counting(Inst.Co), Spatial Relation(Spat.R), Instance Interaction(Inst.It), Visual Reasoning(Vis.R), Text Recognition(Text.R), and both overall accuracy(Overall) and task-level average accuracy(T-Avg.)

Method	Language Model	Vision Model	Overall	LR	AR	RR	FP-S	FP-C	CP
OpenFlamingo	LLaMA 7B	CLIP ViT-L/14	1.7	1.7	4.5	0	1.5	0.8	1.3
MiniGPT-4	Vicuna 7B	EVA-G	11.9	11.6	19.4	5.7	14.6	6.5	10.9
InstructBLIP	Vicuna 7B	EVA-G	23.9	9.2	38.5	16.6	20.9	15	30.8
mPLUG-Owl	LLaMA2 7B	CLIP ViT-L/14	24.9	6.9	34	17.5	33.4	8.5	30.6
VisualGLM	ChatGLM 6B	EVA-CLIP	25.6	5.2	42	18	24.1	13	34.5
LLaVA	LLaMA 7B	CLIP ViT-L/14	36.6	15	52.4	17.1	34.4	27.5	50.3
Qwen-VL-Chat	Qwen-7B	ViT-G/16	56.3	35.3	63.5	46	63.6	43.7	64.7
InternLM-XComposer-VL	InternLM	EVA-G	72.4	44.5	79.5	83.4	71.6	56.3	82.4

Table 6. **Evaluation of MMBench-CN test set.** Here we report the results on the six L-2 abilities based on Chinese, namely Logical Reasoning (LR), Attribute Reasoning (AR), Relation Reasoning (RR), Fine-grained Perception (Cross Instance) (FP-C), Fine-grained Perception (Single Instance) (FP-S), and Coarse Perception (CP).

a caption. Nonetheless, due to limitations in the model’s capacity (e.g., 7B), captions generated by the pre-trained language model often misses the central theme or concept of the article.

To mitigate this challenge, we suggest a supervised fine-tuning approach, utilizing caption data generated via GPT-4. For the creation of this data, GPT-4 is provided with the text-based article and image location, and is instructed to generate a caption that remains coherence with the article’s overarching theme and concept, specifically for image retrieval purposes. Upon data generation, the training data is structured as follows:

< |User| >: [seg<sub>1</sub>][para<sub>1</sub>] ... [seg<sub>N</sub>][para<sub>N</sub>] *Based on the above text, select the appropriate locations for inserting images and give the image captions* <eou>

< |Bot| >: *I think images can be added under the {x<sub>1</sub>}, ..., {x<sub>k</sub>} paragraphs. The image captions are as follows: {x<sub>1</sub>} paragraph: {cap<sub>1</sub>}, ..., {x<sub>k</sub>} paragraph: {cap<sub>k</sub>}* <eob>

Here, [seg<sub>1</sub>] serves as an index token to pinpoint the specific

paragraph index. The placeholders {x<sub>1</sub>} and {x<sub>k</sub>} represent the positions for the first and last image locations, respectively. Correspondingly, {cap<sub>1</sub>} and {cap<sub>k</sub>} act as the generated captions associated with those image locations.

**Image Retrieval and Selection.** Having obtained the captions, a variety of text-image retrieval methods become available for use. In this work, we opt for the CLIP model, capitalizing on its proven efficacy in zero-shot classification tasks. We compute the similarity scores between the generated caption and each image in the candidate pool. The top *m* images, based on these similarity scores, are then selected to constitute the reduced candidate pool for further processing.

To guarantee thematic or conceptual coherence in the images dispersed throughout the article, we deploy our vision-language model to execute the final image selection. When selecting images to accompany the *j*<sup>th</sup> paragraph, the train-

Method	Language Model	Vision Model	Overall	CP	CR	F&C	HF	S&B	SR	TS
OpenFlamingo	LLaMA 7B	CLIP ViT-L/14	0.7	1.8	0	0.8	0	0	2.2	1.5
MiniGPT-4	Vicuna 7B	EVA-G	1.7	7	4	0	0	1	0	0
LLaVA	LLaMA 7B	CLIP ViT-L/14	8.3	10.5	8.1	7.6	1.7	8	11.1	10.6
VisualGLM	ChatGLM 6B	EVA-CLIP	9.2	14	11.1	8.4	0	14	4.4	7.6
InstructBLIP	Vicuna 7B	EVA-G	12.1	8.8	9.1	21	0	12	6.7	18.2
mPLUG-Owl	LLaMA2 7B	CLIP ViT-L/14	12.9	22.8	17.2	6.7	0	25	4.4	7.6
Qwen-VL-Chat	Qwen-7B	ViT-G/16	39.3	40.4	33.3	31.9	3.4	67	51.1	42.4
InternLM-XComposer-VL	InternLM-7B	EVA-G	47.6	50.9	53.5	42	10.3	55	73.3	50

Table 7. **Evaluation of CCBench test set.** Here we report all the sub-tasks, including Calligraphy Painting(CP), Cultural Relic(CR), Food & Clothes(F&C), Historical Figures(H&F), Scenery & Building(S&B), Sketch Reasoning(SR), Traditional Show(TS),

ing data is structured in the following manner:

< |User| >:  $[para_1] \dots [para_i][img_i][para_{i+1}] \dots [para_j]$   
*Based on the given context and candidate*  
*images, select the appropriate image. Candidate*  
*images include:* $[img_j^1] \dots [img_j^m]$  <eou>  
 < |Bot| >: *The {selected index} image.* <eob>

In this configuration,  $[img_i]$  denotes the image associated with the  $i^{th}$  paragraph (preceding the  $j^{th}$  paragraph). The terms  $[img_j^1], \dots, [img_j^m]$  represent the images present in the reduced candidate pool. Meanwhile,  $\{selected\ index\}$  acts as a placeholder indicating the index of the final selected image.

The vision-language model selects images by considering both preceding text and prior images within the article. This mechanism enables the model to acquire an understanding of thematic and visual coherence, an expertise derived from the curated dataset of interleaved image-text compositions.

## 4. Experiments

### 4.1. English-Based Benchmark results.

In this section, we validate the performance of our InternLM-XComposer-VL on several benchmarks.

**MME Benchmark** measures the perception and cognition capability of multi-modality LLMs with carefully crafted questions within 14 sub-tasks. As shown in Table.3, our InternLM-XComposer-VL reached a new state-of-the-art performance 137.11%, outperforms the previous method QWen-VL-Chat with more than 5.0%. We also highlight the Top-3 models within each subtask with underline and we notice that our model reaches the Top-3 performance with 12 of the 14 sub-tasks. This proves the outstanding generalize of our model.

**MMBench** is a hand-crafted challenging benchmark, which evaluates the vision-related reasoning and perception capability with multi-choice questions. The MME Bench

provides both a dev-set and test-set. Here we report the test-set performance of our model. As shown in Table.4. Our method gets 74.4% accuracy and outperforms previous methods by a large margin. Further, our InternLM-XComposer-VL reaches the best performance in 5 of the 6 dimensions. This proves that our model understands the image information well and can handle diverse vision-related tasks.

**Seed-Bench** is a large-scale multi-modality benchmark, which is built with the help of GPT-4 and contains nearly 19K multi-choice questions for both image and video. Here we report the image-set results in Table.5. It can be observed that our InternLM-XComposer-VL gets the best overall performance and the highest performance in 6 of the 9 sub-tasks. We also notice that the sub-task data number is in-balance, for example, the ‘Instance Attributes’ task have 4649 questions, while the ‘Text Understanding’ task only has 84 questions. So the overall metric would be biased toward the tasks that have more questions. To better evaluate the generalized capability of the LLMs along different tasks. We also report the task-level average, similar to the MME benchmark. It can be observed that our model reaches the state-of-the-art average accuracy and outperforms the previous method with 3.3%. This further proves the general capability of our model.

### 4.2. Chinese-Based Benchmark results.

As we introduced in Sec.1, our model is pretrained with rich multilingual knowledge. To prove the effectiveness of the pretraining, here we further evaluate its performance with two Chinese-based benchmarks.

**MMBench-CN** is the Chinese translated benchmark of the original MMBench, which shows the vision-related Chinese understanding and reasoning capability. Here we report the test-set performance in Table.6. It can be observed that our method outperforms previous methods by a large margin. When comparing with the English version performance in Table.4. Qwen and VisualGLM have 4.9% and 7.9% performance degrading, while the performance gap of our model between different languages is only 2.0%. This proves the

strong multi-lingo capability of our model.

**Chinese-Bench** is a Chinese knowledge-related benchmark, that challenges the model with Chinese traditional cultural questions, including art, food, clothes, landmarks, *etc.* Here we report the performance in Table.7. It can be observed that the benchmark is quite challenging, most LLaMA-based model fails to answer these questions, due to the lack of corresponding knowledge. Compared with LLaMA-based methods, the QWen-based model Qwen-VL-Chat shows a much better performance of 39.3%. While it is still worse than our InternLM-based model InternLM-XComposer-VL, which reaches a new state-of-the-art performance of 47.6%. This proves the rich Chinese knowledge of InternLM and the great alignment between the vision and language knowledge by our large-scale pre-training.

## 5. Conclusion and Outlook

In this paper, we present InternLM-XComposer, a vision-language large model with superb multi-modality understanding and composition capability. Benefiting from the rich multi-lingual and multi-modality knowledge from our carefully designed pretraining, on one hand, our model could generate coherent and contextual articles with a simple title input, and integrate images at the proper location and content. On the other hand, our model shows state-of-the-art performance across various mainstream vision-language LLM benchmarks. We hope our InternLM-XComposer could provide new insight for the following exploration of advanced vision-language interaction.

## References

- [1] Stanislaw Antol, Aishwarya Agrawal, Jiasen Lu, Margaret Mitchell, Dhruv Batra, C. Lawrence Zitnick, and Devi Parikh. Vqa: Visual question answering. In *International Conference on Computer Vision (ICCV)*, 2015. 5
- [2] Anas Awadalla, Irena Gao, Josh Gardner, Jack Hessel, Yusuf Hanafy, Wanrong Zhu, Kalyani Marathe, Yonatan Bitton, Samir Gadre, Shiori Sagawa, Jenia Jitsev, Simon Kornblith, Pang Wei Koh, Gabriel Ilharco, Mitchell Wortsman, and Ludwig Schmidt. Openflamingo: An open-source framework for training large autoregressive vision-language models. *arXiv.org*, 2023. 3
- [3] Jinze Bai, Shuai Bai, Shusheng Yang, Shijie Wang, Sinan Tan, Peng Wang, Junyang Lin, Chang Zhou, and Jingren Zhou. Qwen-vl: A frontier large vision-language model with versatile abilities. *arXiv.org*, 2023. 3, 7
- [4] Baichuan. Baichuan 2: Open large-scale language models. *arXiv.org*, 2023. 2
- [5] Tom Brown, Benjamin Mann, Nick Ryder, Melanie Subbiah, Jared D Kaplan, Prafulla Dhariwal, Arvind Neelakantan, Pranav Shyam, Girish Sastry, Amanda Askell, et al. Language models are few-shot learners. *Advances in Neural Information Processing Systems (NeurIPS)*, 33:1877–1901, 2020. 2
- [6] Soravit Changpinyo, Piyush Sharma, Nan Ding, and Radu Soricut. Conceptual 12m: Pushing web-scale image-text pre-training to recognize long-tail visual concepts. In *Proceedings of the IEEE/CVF Conference on Computer Vision and Pattern Recognition*, pages 3558–3568, 2021. 5
- [7] Keqin Chen, Zhao Zhang, Weili Zeng, Richong Zhang, Feng Zhu, and Rui Zhao. Shikra: Unleashing multimodal llm’s referential dialogue magic. *arXiv.org*, 2023. 3
- [8] Xinlei Chen, Hao Fang, Tsung-Yi Lin, Ramakrishna Vedantam, Saurabh Gupta, Piotr Dollar, and C. Lawrence Zitnick. Microsoft coco captions: Data collection and evaluation server, 2015. 5
- [9] Wei-Lin Chiang, Zhuohan Li, Zi Lin, Ying Sheng, Zhanghao Wu, Hao Zhang, Lianmin Zheng, Siyuan Zhuang, Yonghao Zhuang, Joseph E. Gonzalez, Ion Stoica, and Eric P. Xing. Vicuna: An open-source chatbot impressing gpt-4 with 90%\* chatgpt quality, March 2023. 2, 3
- [10] Aakanksha Chowdhery, Sharan Narang, Jacob Devlin, Maarten Bosma, Gaurav Mishra, Adam Roberts, Paul Barham, Hyung Won Chung, Charles Sutton, Sebastian Gehrmann, et al. Palm: Scaling language modeling with pathways. *arXiv.org*, 2022. 2
- [11] Wenliang Dai, Junnan Li, Dongxu Li, Anthony Meng Huat Tiong, Junqi Zhao, Weisheng Wang, Boyang Li, Pascale Fung, and Steven Hoi. Instructblip: Towards general-purpose vision-language models with instruction tuning, 2023. 2, 3, 7
- [12] Abhishek Das, Satwik Kottur, Khushi Gupta, Avi Singh, Deshraj Yadav, José MF Moura, Devi Parikh, and Dhruv Batra. Visual dialog. In *Proceedings of the IEEE conference on computer vision and pattern recognition*, pages 326–335, 2017. 5

- [13] Jia Deng, Wei Dong, Richard Socher, Li-Jia Li, Kai Li, and Li Fei-Fei. Imagenet: A large-scale hierarchical image database. In *Proceedings of the IEEE/CVF Conference on Computer Vision and Pattern Recognition (CVPR)*, pages 248–255, 2009. 3
- [14] Jacob Devlin, Ming-Wei Chang, Kenton Lee, and Kristina Toutanova. Bert: Pre-training of deep bidirectional transformers for language understanding. *arXiv.org*, 2018. 2, 4
- [15] Danny Driess, Fei Xia, Mehdi S. M. Sajjadi, Corey Lynch, Aakanksha Chowdhery, Brian Ichter, Ayzaan Wahid, Jonathan Tompson, Quan Vuong, Tianhe Yu, Wenlong Huang, Yevgen Chebotar, Pierre Sermanet, Daniel Duckworth, Sergey Levine, Vincent Vanhoucke, Karol Hausman, Marc Toussaint, Klaus Greff, Andy Zeng, Igor Mordatch, and Pete Florence. Palm-e: An embodied multimodal language model. In *arXiv preprint arXiv:2303.03378*, 2023. 2
- [16] Zhengxiao Du, Yujie Qian, Xiao Liu, Ming Ding, Jiezhong Qiu, Zhilin Yang, and Jie Tang. Gln: General language model pretraining with autoregressive blank infilling. In *Proceedings of the 60th Annual Meeting of the Association for Computational Linguistics (Volume 1: Long Papers)*, pages 320–335, 2022. 2, 7
- [17] Yuxin Fang, Wen Wang, Binhui Xie, Quan Sun, Ledell Wu, Xinggang Wang, Tiejun Huang, Xinlong Wang, and Yue Cao. Eva: Exploring the limits of masked visual representation learning at scale. In *Proceedings of the IEEE/CVF Conference on Computer Vision and Pattern Recognition (CVPR)*, pages 19358–19369, 2023. 3, 4
- [18] Chaoyou Fu, Peixian Chen, Yunhang Shen, Yulei Qin, Mengdan Zhang, Xu Lin, Zhenyu Qiu, Wei Lin, Jinrui Yang, Xiawu Zheng, Ke Li, Xing Sun, and Rongrong Ji. Mme: A comprehensive evaluation benchmark for multimodal large language models. *arXiv preprint arXiv:2306.13394*, 2023. 2
- [19] Peng Gao, Jiaming Han, Renrui Zhang, Ziyi Lin, Shijie Geng, Aojun Zhou, W. Zhang, Pan Lu, Conghui He, Xiangyu Yue, Hongsheng Li, and Yu Jiao Qiao. Llama-adapter v2: Parameter-efficient visual instruction model. *ArXiv*, abs/2304.15010, 2023. 7
- [20] Tao Gong, Chengqi Lyu, Shilong Zhang, Yudong Wang, Miao Zheng, Qianmengke Zhao, Kuikun Liu, Wenwei Zhang, Ping Luo, and Kai Chen. Multimodal-gpt: A vision and language model for dialogue with humans. *ArXiv*, abs/2305.04790, 2023. 7
- [21] Jiayi Gu, Xiaojun Meng, Guansong Lu, Lu Hou, Niu Minzhe, Xiaodan Liang, Lewei Yao, Runhui Huang, Wei Zhang, Xin Jiang, et al. Wukong: A 100 million large-scale chinese cross-modal pre-training benchmark. *Advances in Neural Information Processing Systems*, 35:26418–26431, 2022. 5
- [22] Conghui He, Zhenjiang Jin, Chaoxi Xu, Jiantao Qiu, Bin Wang, Wei Li, Hang Yan, Jiaqi Wang, and Da Lin. Wanjuan: A comprehensive multimodal dataset for advancing english and chinese large models. *ArXiv*, abs/2308.10755, 2023. 5
- [23] Edward J Hu, Yelong Shen, Phillip Wallis, Zeyuan Allen-Zhu, Yuanzhi Li, Shean Wang, Lu Wang, and Weizhu Chen. LoRA: Low-rank adaptation of large language models. In *International Conference on Learning Representations*, 2022. 3, 5
- [24] W. Hu, Y. Xu, Y. Li, W. Li, Z. Chen, and Z. Tu. Bliva: A simple multimodal llm for better handling of text-rich visual questions. *ArXiv*, abs/2308.09936, 2023. 7
- [25] Ziniu Hu, Ahmet Iscen, Chen Sun, Zirui Wang, Kai-Wei Chang, Yizhou Sun, Cordelia Schmid, David A Ross, and Alireza Fathi. Reveal: Retrieval-augmented visual-language pre-training with multi-source multimodal knowledge memory. In *Proceedings of the IEEE/CVF Conference on Computer Vision and Pattern Recognition (CVPR)*, pages 23369–23379, 2023. 3
- [26] Drew A Hudson and Christopher D Manning. Gqa: A new dataset for real-world visual reasoning and compositional question answering. *Conference on Computer Vision and Pattern Recognition (CVPR)*, 2019. 5
- [27] Chao Jia, Yinfei Yang, Ye Xia, Yi-Ting Chen, Zarana Parekh, Hieu Pham, Quoc Le, Yun-Hsuan Sung, Zhen Li, and Tom Duerig. Scaling up visual and vision-language representation learning with noisy text supervision. In *Proceedings of the International Conference on Machine learning (ICML)*, pages 4904–4916. PMLR, 2021. 3
- [28] Jing Yu Koh, Ruslan Salakhutdinov, and Daniel Fried. Grounding language models to images for multimodal inputs and outputs. 2023. 3
- [29] Bohao Li, Rui Wang, Guangzhi Wang, Yuying Ge, Yixiao Ge, and Ying Shan. Seed-bench: Benchmarking multimodal llms with generative comprehension, 2023. 2
- [30] Bo Li, Yuanhan Zhang, Liangyu Chen, Jinghao Wang, Jingkang Yang, and Ziwei Liu. Otter: A multi-modal model with in-context instruction tuning. *arXiv.org*, 2023. 3, 7
- [31] Junnan Li, Dongxu Li, Silvio Savarese, and Steven C. H. Hoi. Blip-2: Bootstrapping language-image pre-training with frozen image encoders and large language models. *ArXiv*, abs/2301.12597, 2023. 2, 4, 7
- [32] Junnan Li, Dongxu Li, Caiming Xiong, and Steven Hoi. Blip: Bootstrapping language-image pre-training for unified vision-language understanding and generation. In *Proceedings of the International Conference on Machine learning (ICML)*, pages 12888–12900. PMLR, 2022. 3
- [33] Juncheng Li, Kaihang Pan, Zhiqi Ge, Minghe Gao, Hanwang Zhang, Wei Ji, Wenqiao Zhang, Tat-Seng Chua, Siliang Tang, and Yueting Zhuang. Empowering vision-language models to follow interleaved vision-language instructions. *ArXiv*, abs/2308.04152, 2023. 7
- [34] Liunian Harold Li\*, Pengchuan Zhang\*, Haotian Zhang\*, Jianwei Yang, Chunyuan Li, Yiwu Zhong, Lijuan Wang, Lu Yuan, Lei Zhang, Jenq-Neng Hwang, Kai-Wei Chang, and Jianfeng Gao. Grounded language-image pre-training. In *Proceedings of the IEEE/CVF Conference on Computer Vision and Pattern Recognition (CVPR)*, 2022. 3
- [35] Fangyu Liu, Guy Edward Toh Emerson, and Nigel Collier. Visual spatial reasoning. *Transactions of the Association for Computational Linguistics*, 2023. 5
- [36] Fuxiao Liu, Kevin Lin, Linjie Li, Jianfeng Wang, Yaser Yacoob, and Lijuan Wang. Aligning large multi-modal model with robust instruction tuning. *arXiv preprint arXiv:2306.14565*, 2023. 5

- [37] Fuxiao Liu, Kevin Lin, Linjie Li, Jianfeng Wang, Yaser Yacoob, and Lijuan Wang. Mitigating hallucination in large multi-modal models via robust instruction tuning. 2023. [7](#)
- [38] Haotian Liu, Chunyuan Li, Qingyang Wu, and Yong Jae Lee. Visual instruction tuning. *arXiv.org*, 2023. [2](#), [3](#), [5](#), [7](#)
- [39] Shilong Liu, Zhaoyang Zeng, Tianhe Ren, Feng Li, Hao Zhang, Jie Yang, Chunyuan Li, Jianwei Yang, Hang Su, Jun Zhu, et al. Grounding dino: Marrying dino with grounded pre-training for open-set object detection. *arXiv.org*, 2023. [3](#)
- [40] Yulong Liu, Guibo Zhu, Bin Zhu, Qi Song, Guojing Ge, Haoran Chen, GuanHui Qiao, Ru Peng, Lingxiang Wu, and Jinqiao Wang. Taisu: A 166m large-scale high-quality dataset for chinese vision-language pre-training. *Advances in Neural Information Processing Systems*, 35:16705–16717, 2022. [5](#)
- [41] Pan Lu, Swaroop Mishra, Tanglin Xia, Liang Qiu, Kai-Wei Chang, Song-Chun Zhu, Oyvind Tafjord, Peter Clark, and Ashwin Kalyan. Learn to explain: Multimodal reasoning via thought chains for science question answering. *Advances in Neural Information Processing Systems*, 35:2507–2521, 2022. [5](#)
- [42] Pan Lu, Liang Qiu, Jiaqi Chen, Tony Xia, Yizhou Zhao, Wei Zhang, Zhou Yu, Xiaodan Liang, and Song-Chun Zhu. Iconqa: A new benchmark for abstract diagram understanding and visual language reasoning. *arXiv preprint arXiv:2110.13214*, 2021. [5](#)
- [43] Gen Luo, Yiyi Zhou, Tianhe Ren, Shen Chen, Xiaoshuai Sun, and Rongrong Ji. Cheap and quick: Efficient vision-language instruction tuning for large language models. *ArXiv*, abs/2305.15023, 2023. [7](#)
- [44] Kenneth Marino, Mohammad Rastegari, Ali Farhadi, and Roozbeh Mottaghi. Ok-vqa: A visual question answering benchmark requiring external knowledge. In *Proceedings of the IEEE/cvf conference on computer vision and pattern recognition*, pages 3195–3204, 2019. [5](#)
- [45] Anand Mishra, Shashank Shekhar, Ajeet Kumar Singh, and Anirban Chakraborty. Ocr-vqa: Visual question answering by reading text in images. In *ICDAR*, 2019. [5](#)
- [46] OpenAI. Chatgpt. <https://openai.com/blog/chatgpt>, 2022. [2](#)
- [47] OpenAI. Gpt-4 technical report, 2023. [2](#)
- [48] Vicente Ordonez, Girish Kulkarni, and Tamara L. Berg. Im2text: Describing images using 1 million captioned photographs. In *Neural Information Processing Systems (NIPS)*, 2011. [5](#)
- [49] Long Ouyang, Jeffrey Wu, Xu Jiang, Diogo Almeida, Carroll Wainwright, Pamela Mishkin, Chong Zhang, Sandhini Agarwal, Katarina Slama, Alex Ray, et al. Training language models to follow instructions with human feedback. *Advances in Neural Information Processing Systems (NeurIPS)*, 35:27730–27744, 2022. [2](#)
- [50] Zhiliang Peng, Wenhui Wang, Li Dong, Yaru Hao, Shaohan Huang, Shuming Ma, and Furu Wei. Kosmos-2: Grounding multimodal large language models to the world. *arXiv.org*, 2023. [3](#)
- [51] Qwen. Introducing qwen-7b: Open foundation and human-aligned models (of the state-of-the-arts), 2023. [2](#)
- [52] Alec Radford, Jong Wook Kim, Chris Hallacy, Aditya Ramesh, Gabriel Goh, Sandhini Agarwal, Girish Sastry, Amanda Askell, Pamela Mishkin, Jack Clark, et al. Learning transferable visual models from natural language supervision. In *Proceedings of the International Conference on Machine learning (ICML)*, pages 8748–8763. PMLR, 2021. [2](#), [3](#)
- [53] Alec Radford, Karthik Narasimhan, Tim Salimans, Ilya Sutskever, et al. Improving language understanding by generative pre-training. 2018. [2](#)
- [54] Colin Raffel, Noam Shazeer, Adam Roberts, Katherine Lee, Sharan Narang, Michael Matena, Yanqi Zhou, Wei Li, and Peter J Liu. Exploring the limits of transfer learning with a unified text-to-text transformer. *Journal of Machine Learning Research (JMLR)*, 21(1):5485–5551, 2020. [2](#)
- [55] Christoph Schuhmann, Romain Beaumont, Richard Vencu, Cade Gordon, Ross Wightman, Mehdi Cherti, Theo Coombes, Aarush Katta, Clayton Mullis, Mitchell Wortsman, et al. Laion-5b: An open large-scale dataset for training next generation image-text models. *Advances in Neural Information Processing Systems*, 35:25278–25294, 2022. [5](#)
- [56] Christoph Schuhmann, Richard Vencu, Romain Beaumont, Robert Kaczmarczyk, Clayton Mullis, Aarush Katta, Theo Coombes, Jenia Jitsev, and Aran Komatsuzaki. Laion-400m: Open dataset of clip-filtered 400 million image-text pairs. *arXiv preprint arXiv:2111.02114*, 2021. [5](#)
- [57] Dustin Schwenk, Apoorv Khandelwal, Christopher Clark, Kenneth Marino, and Roozbeh Mottaghi. A-okvqa: A benchmark for visual question answering using world knowledge. In *European Conference on Computer Vision*, pages 146–162. Springer, 2022. [5](#)
- [58] Piyush Sharma, Nan Ding, Sebastian Goodman, and Radu Soricut. Conceptual captions: A cleaned, hypernymed, image alt-text dataset for automatic image captioning. In *Proceedings of the 56th Annual Meeting of the Association for Computational Linguistics (Volume 1: Long Papers)*, pages 2556–2565, 2018. [5](#)
- [59] Oleksii Sidorov, Ronghang Hu, Marcus Rohrbach, and Amanpreet Singh. Textcaps: a dataset for image captioning with reading comprehension. In *Computer Vision—ECCV 2020: 16th European Conference, Glasgow, UK, August 23–28, 2020, Proceedings, Part II 16*, pages 742–758. Springer, 2020. [5](#)
- [60] Amanpreet Singh, Vivek Natarajan, Meet Shah, Yu Jiang, Xinlei Chen, Dhruv Batra, Devi Parikh, and Marcus Rohrbach. Towards vqa models that can read. In *Proceedings of the IEEE/CVF conference on computer vision and pattern recognition*, pages 8317–8326, 2019. [5](#)
- [61] Rohan Taori, Ishaan Gulrajani, Tianyi Zhang, Yann Dubois, Xuechen Li, Carlos Guestrin, Percy Liang, and Tatsunori B. Hashimoto. Stanford alpaca: An instruction-following llama model. [https://github.com/tatsu-lab/stanford\\_alpaca](https://github.com/tatsu-lab/stanford_alpaca), 2023. [5](#)
- [62] InternLM Team. Internlm: A multilingual language model with progressively enhanced capabilities. <https://github.com/InternLM/InternLM>, 2023. [2](#), [4](#)
- [63] Hugo Touvron, Thibaut Lavril, Gautier Izacard, Xavier Martinet, Marie-Anne Lachaux, Timothée Lacroix, Baptiste

- Rozière, Naman Goyal, Eric Hambro, Faisal Azhar, et al. Llama: Open and efficient foundation language models. *arXiv.org*, 2023. [2](#)
- [64] Hugo Touvron, Louis Martin, Kevin Stone, Peter Albert, Amjad Almahairi, Yasmine Babaei, Nikolay Bashlykov, Soumya Batra, Prajjwal Bhargava, Shruti Bhosale, et al. Llama 2: Open foundation and fine-tuned chat models, 2023. [2](#)
- [65] Ashish Vaswani, Noam Shazeer, Niki Parmar, Jakob Uszkoreit, Llion Jones, Aidan N Gomez, Łukasz Kaiser, and Illia Polosukhin. Attention is all you need. *Advances in Neural Information Processing Systems (NeurIPS)*, 30, 2017. [2](#)
- [66] Bin Wang, Fan Wu, Xiao Han, Jiahui Peng, Huaping Zhong, Pan Zhang, Xiaoyi Dong, Weijia Li, Wei Li, Jiaqi Wang, et al. Vigc: Visual instruction generation and correction. *arXiv.org*, 2023. [3](#)
- [67] Jianfeng Wang, Zhengyuan Yang, Xiaowei Hu, Linjie Li, Kevin Lin, Zhe Gan, Zicheng Liu, Ce Liu, and Lijuan Wang. Git: A generative image-to-text transformer for vision and language. *ArXiv*, abs/2205.14100, 2022. [7](#)
- [68] An Yang, Junshu Pan, Junyang Lin, Rui Men, Yichang Zhang, Jingren Zhou, and Chang Zhou. Chinese clip: Contrastive vision-language pretraining in chinese. *arXiv.org*, 2022. [2](#), [4](#), [5](#)
- [69] Michihiro Yasunaga, Armen Aghajanyan, Weijia Shi, Richard James, Jure Leskovec, Percy Liang, Mike Lewis, Luke Zettlemoyer, and Wen-tau Yih. Retrieval-augmented multimodal language modeling. 2023. [3](#)
- [70] Qinghao Ye, Haiyang Xu, Guohai Xu, Jiabo Ye, Ming Yan, Yiyang Zhou, Junyang Wang, Anwen Hu, Pengcheng Shi, Yaya Shi, et al. mplug-owl: Modularization empowers large language models with multimodality. *arXiv.org*, 2023. [3](#), [7](#)
- [71] Shukang Yin, Chaoyou Fu, Sirui Zhao, Ke Li, Xing Sun, Tong Xu, and Enhong Chen. A survey on multimodal large language models. *arXiv preprint arXiv:2306.13549*, 2023. [2](#)
- [72] Yuanhan Zhang Bo Li Songyang Zhnag Wangbo Zhao Yike Yuan Jiaqi Wang Conghui He Ziwei Liu Kai Chen Dahua Lin Yuan Liu, Haodong Duan. Mmbench: Is your multi-modal model an all-around player? *arXiv:2307.06281*, 2023. [2](#)
- [73] Yan Zeng, Hanbo Zhang, Jiani Zheng, Jiangnan Xia, Guoqiang Wei, Yang Wei, Yuchen Zhang, and Tao Kong. What matters in training a gpt4-style language model with multimodal inputs? *ArXiv*, abs/2307.02469, 2023. [7](#)
- [74] Haotian Zhang, Pengchuan Zhang, Xiaowei Hu, Yen-Chun Chen, Liunian Li, Xiyang Dai, Lijuan Wang, Lu Yuan, Jenq-Neng Hwang, and Jianfeng Gao. Glipv2: Unifying localization and vision-language understanding. *Advances in Neural Information Processing Systems (NeurIPS)*, 35:36067–36080, 2022. [3](#)
- [75] Susan Zhang, Stephen Roller, Naman Goyal, Mikel Artetxe, Moya Chen, Shuohui Chen, Christopher Dewan, Mona Diab, Xian Li, Xi Victoria Lin, et al. Opt: Open pre-trained transformer language models, 2022. *arXiv.org*. [3](#)
- [76] Haozhe Zhao, Zefan Cai, Shuzheng Si, Xiaojian Ma, Kaikai An, Liang Chen, Zixuan Liu, Sheng Wang, Wenjuan Han, and Baobao Chang. Mmicl: Empowering vision-language model with multi-modal in-context learning. *arXiv.org*, 2023. [3](#)
- [77] Haozhe Zhao, Zefan Cai, Shuzheng Si, Xiaojian Ma, Kaikai An, Liang Chen, Zixuan Liu, Sheng Wang, Wenjuan Han, and Baobao Chang. Mmicl: Empowering vision-language model with multi-modal in-context learning. *ArXiv*, abs/2309.07915, 2023. [7](#)
- [78] Zhiyuan Zhao, Linke Ouyang, Bin Wang, Siyuan Huang, Pan Zhang, Xiaoyi Dong, Jiaqi Wang, and Conghui He. Mllm-dataengine: An iterative refinement approach for mllm. *arXiv.org*, 2023. [3](#)
- [79] Deyao Zhu, Jun Chen, Xiaoqian Shen, Xiang Li, and Mohamed Elhoseiny. Minigpt-4: Enhancing vision-language understanding with advanced large language models. *arXiv.org*, 2023. [2](#), [3](#), [7](#)
- [80] Wanrong Zhu, Jack Hessel, Anas Awadalla, Samir Yitzhak Gadre, Jesse Dodge, Alex Fang, Youngjae Yu, Ludwig Schmidt, William Yang Wang, and Yejin Choi. Multimodal c4: An open, billion-scale corpus of images interleaved with text. *arXiv preprint arXiv:2304.06939*, 2023. [5](#)

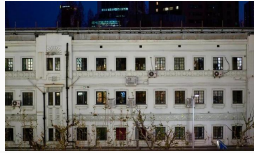
## Shanghai Travel Guide

Shanghai is the largest city in China and one of the most populous cities in the world, with a population of over 24 million people. The city is known for its modern skyscrapers, bustling financial district, and vibrant nightlife. Shanghai is also home to some of the country's top tourist attractions, including the Bund, Yuyuan Garden, and the Oriental Pearl Tower. In this guide, we'll provide you with all the information you need to plan your trip to Shanghai, including tips on where to stay, what to do, and how to get around.



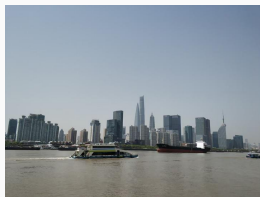
### Where to Stay in Shanghai

When it comes to finding a place to stay in Shanghai, there are plenty of options to choose from. If you're looking for a luxury experience, consider staying at one of the city's five-star hotels, such as the Fairmont Peace Hotel or the Waldorf Astoria Shanghai on the Bund. These hotels offer stunning views of the city skyline, luxurious amenities, and impeccable service.



If you're looking for something more budget-friendly, there are plenty of hostels and guesthouses throughout the city that offer affordable accommodations. Some popular areas to stay include the Xintiandi neighborhood, which is known for its trendy bars and restaurants, and the French Concession, which is filled with charming cafes and boutiques.

### What to Do in Shanghai



One of the best ways to explore Shanghai is by taking a stroll along the Bund, a waterfront promenade that offers stunning views of the city skyline. You can also visit the Yu Garden, a traditional Chinese garden that dates back to the Ming Dynasty, and the Shanghai Museum, which houses an impressive collection of Chinese art and artifacts.

Another popular attraction in Shanghai is the Oriental Pearl Tower, a television tower that offers panoramic views of the city. You can also take a boat ride on the Huangpu River, which runs through the heart of the city, and visit the Jade Buddha Temple, a Buddhist temple that houses two jade Buddha statues.



### How to Get Around in Shanghai

The best way to get around Shanghai is by using public transportation, which includes buses, subways, and taxis. The city's subway system is extensive and easy to use, with stations located throughout the city. Buses are also a convenient way to get around, although they can be crowded during rush hour.



Taxis are available throughout the city, but make sure to agree on a price before getting into the taxi so you don't get ripped off. Another option is to rent a bicycle or scooter, which will allow you to explore the city at your own pace.

### Tips for Visiting Shanghai



1. Dress appropriately: Shanghai is a conservative city, so it's important to dress modestly when visiting temples and other religious sites. Cover your shoulders and knees, and avoid wearing revealing clothing.

2. Learn some basic Mandarin: While many people in Shanghai speak English, it's always helpful to know some basic Mandarin phrases, such as "hello," "thank you," and "excuse me."



3. Be aware of pickpockets: Like any major city, Shanghai has its fair share of pickpockets. Keep your valuables close to you and be vigilant about your surroundings.

...

In conclusion, Shanghai is a vibrant and exciting city that offers something for everyone. Whether you're interested in history, culture, or just want to have a good time, Shanghai has it all. With its towering skyscrapers, bustling streets, and rich cultural heritage, Shanghai is a must-visit destination for anyone traveling to China.



## 又见敦煌

敦煌，位于甘肃省西北部，地处河西走廊西端，是古代丝绸之路上的重要交通枢纽和商埠重镇。它拥有着丰富的历史文化遗产，包括莫高窟、鸣沙山月牙泉、雅丹魔鬼城等著名景点。同时，敦煌也是中国历史文化名城之一，有着深厚的文化底蕴和独特的民俗风情。



### 一、莫高窟

莫高窟，又名“千佛洞”，是中国四大石窟之一，始建于十六国的前秦时期，距今已有1600多年的历史。它是世界上现存规模最大、内容最丰富的佛教艺术宝库，被誉为“东方卢浮宫”。莫高窟内共有735个洞窟，壁画总面积达45000多平方米，彩塑佛像5000余尊，是世界上最大的佛教艺术中心之一。在这里，游客可以欣赏到精美的壁画、雕塑和音乐表演，感受佛教文化的博大精深。



### 二、鸣沙山月牙泉

鸣沙山月牙泉是一处自然奇观，位于敦煌市西北约40公里处的沙漠中。这里地势平坦，沙丘连绵起伏，形成了一片广袤无垠的沙漠景观。而月牙泉则静静地镶嵌在这片沙漠之中，泉水清澈见底，形状如新月，故称“月牙泉”。每到夜晚，月亮升起时，月牙泉周围会发出阵阵清脆的响声，犹如天籁之音，令人心旷神怡。



### 三、雅丹魔鬼城

雅丹魔鬼城是一座典型的风蚀地貌，位于敦煌市西南约100公里的戈壁滩上。这里的地貌奇特，呈现出一种荒凉、

神秘、恐怖的景象。由于长期受到风吹日晒雨淋，这里的岩石表面已经变得凹凸不平，形成了各种形态各异的造型，有的像动物，有的像人物，有的像建筑，让人不禁感叹大自然的鬼斧神工。



### 四、其他景点

除了莫高窟、鸣沙山月牙泉和雅丹魔鬼城之外，敦煌还有许多其他值得一游的景点，如玉门关、阳关、锁阳城、汉长城遗址等。这些景点都具有悠久的历史和文化价值，吸引着众多游客前来参观游览。



### 五、特色美食

敦煌的特色美食也非常丰富，其中最著名的当属驴肉黄面了。驴肉黄面是一道以驴肉为主要食材的面食，味道鲜香可口，深受当地人和游客的喜爱。此外，还有羊肉泡馍、胡羊焖饼、烤全羊等特色美食，都是不容错过的美味佳肴。



### 六、旅游小贴士

1. 敦煌气候干燥，日照强烈，紫外线较强，建议游客做好防晒措施，携带防晒霜、遮阳帽、太阳镜等物品。2. 敦煌属于高原地区，海拔较高，游客应注意休息，避免剧烈运动，以免出现高原反应。3. 敦煌旅游景点较多，游客应提前规划好行程，合理安排时间，避免走马观花，错过重要的景点。4. 在敦煌旅游期间，要注意保护环境，不乱扔垃圾，不破坏文物古迹，做一个文明的游客。总之，敦煌是一座历史悠久、文化底蕴深厚、风景优美的城市，是一个值得一游的好去处。希望这篇文章能够帮助您更好地了解敦煌，为您的旅行提供一些有用的信息。

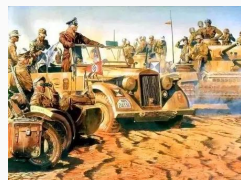
## The World War 2

World War II (WWII or WW2), also known as the Second World War, was a global war that lasted from 1939 to 1945. It involved the vast majority of the world's countries—including all of the great powers—eventually forming two opposing military alliances: the Allies and the Axis.



It was the most widespread war in history, with some 100 million military personnel, including 60 million on the Allied side and 30 million on the Axis side, participating in more than 5,000 air battles, land battles, and naval engagements in 60 countries across five continents.

On September 1, 1939, Germany invaded Poland, marking the start of Operation Barbarossa, the German invasion of the Soviet Union. On December 7, 1941, Japan launched a surprise attack on Pearl Harbor, Hawaii, resulting in the United States' entry into the war on the side of the Allies.



In June 1941, Nazi Germany invaded the Soviet Union during Operation Barbarossa. This marked the beginning of the largest tank battle in history, the Battle of Kursk, which took place between July 12 and August 23, 1943. The Soviets were able to inflict heavy losses on the Germans, forcing them to retreat back to their original positions.

The Battle of Stalingrad, which took place between August 1942 and February 1943, was one of the bloodiest battles in human history. During this time, the Red Army suffered an estimated 900,000 casualties, while the Wehrmacht lost approximately 600,000 soldiers.



The Battle of El Alamein, which took place between October 1942 and November 1943, was another major turning point in the war. Here, the British Eighth Army under General Bernard Montgomery defeated the German Afrika Korps led by Field Marshal Erwin Rommel at the Sidi Rezegh Pass near Tobruk, Libya.

This victory allowed the Allies to gain control of much of North Africa and paved the way for the eventual defeat of Adolf Hitler's forces in Europe.



The Battle of Midway, which took place between June 4-7, 1942, saw the U.S. Navy decisively defeat the Imperial Japanese Navy off the coast of Midway Atoll in the Pacific Ocean. This victory helped turn the tide of the war in favor of the Allies.

The Battle of Normandy, which took place between June 6-July 29, 1944, was the largest amphibious invasion in history. Over 160,000 Allied troops landed on the beaches of Normandy, France, supported by over 10,000 aircraft and nearly 5,000 landing craft.



After several weeks of fierce fighting, the Allies had secured a foothold in France and were able to begin advancing towards Germany.

The Battle of the Bulge, which took place between December 16, 1944, and January 25, 1945, was a last-ditch attempt by the German army to break through the Allied lines and end the war before it could be officially declared.



Despite being outnumbered and outgunned, the Allies were able to repel the German offensive and continue their advance towards Germany.

The Battle of Okinawa, which took place between April 1-May 22, 1945, was the final major battle of the Pacific Theater of World War II.



Here, the U.S. Marine Corps and the Ryukyu Islands Defense Force fought against the Imperial Japanese Army until the latter surrendered unconditionally on August 14, 1945.

The atomic bombings of Hiroshima and Nagasaki, which took place on August 6 and August 9, 1945, respectively, marked the first use of nuclear weapons in warfare.



These bombings resulted in the immediate deaths of tens of thousands of people and contributed to the rapid conclusion of the war.

Overall, World War II is remembered as one of the deadliest conflicts in human history, claiming the lives of millions of men, women, and children around the world.

## C919宣传广告

C919大型客机是中国自行研制、具有自主知识产权的大型喷气式民用飞机，座级158-168人，航程4075-5555公里。2017年5月14日，国产大飞机C919在上海浦东国际机场首飞成功！这是中国航空工业发展史上的一个重要里程碑，标志着我国成为继美国、俄罗斯之后世界上第三个能够设计制造大型客机的国家。



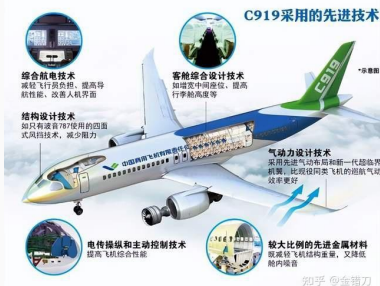
### 1. C919的研发历程

1999年12月22日，国务院正式批准了中国商用飞机有限责任公司（COMAC）筹建；2002年6月29日，中俄两国政府在北京签署了关于联合研制和生产新型干线宽体客机的合作意向书；2003年9月25日，在人民大会堂举行了隆重的签字仪式；



2010年4月26日，第一架C919原型机在中国上海总装下线并进行了首次地面滑行试车（即“一地两检”）；同年11月30日，第二架C919完成全机静力试验并获得型号合格证（TC）；2018年02月28日，第三架C919顺利通过适航取证审定试飞并在北京首都机场着陆后转场至西安阎良进行交付前的系统调试与性能优化工作。

### 2. C919的主要特点



**安全性高：**由于采用了先进的设计理念和技术手段，使得该机型具有良好的抗坠毁性以及超强的防冰雨雪能力等优点；此外它还配备了先进的电子飞行仪表系统和自动驾驶仪以提高飞行员操作效率降低人为因素对飞行安全造成影响等等一系列措施都为保证乘客生命财产安全提供了有力保障！

**舒适性好：**为了满足多层次旅客需求而专门开发出符合人体工程学原理设计的经济舱座椅不仅美观大方而且坐起

来也非常舒服哦！另外还有宽敞明亮且视野开阔的全景式舷窗可以随时欣赏到窗外美丽景色呢~总之一句话概括就是两个字——高大上啊哈哈^\_^!!

**节能环保：**作为一款绿色出行交通工具当然不能落后于时代潮流啦对吧？所以设计师们在设计之初就充分考虑到这一点并将其融入了整个机身结构当中从而大大降低了燃油消耗量同时还能有效减少尾气排放污染环境保护我们赖以生存的大好河山哟o(\*^▽^\*)o!!以上便是小编为大家整理出来的全部内容希望对您有所帮助如果您还有其他疑问或者想了解更多相关资讯请继续关注本号后续推送文章敬请期待吧٩(●>▽<)〃(´ε`)-☆

## 星链新闻稿

北京时间2021年9月13日，星链（Starlink）在美国内华达州拉斯维加斯举行的第52届国际消费电子展（CES 2021）上展示了其卫星互联网服务。



在展会现场，SpaceX公司首席执行官埃隆·马斯克（Elon Musk）向与会者介绍了星链的最新进展和计划。他表示，星链将为全球提供高速、低延迟的网络接入服务，并将在未来几年内覆盖全球大部分地区。

据介绍，星链是一个由近1.2万颗通信卫星组成的系统，这些卫星分布在多个轨道上，以实现全球覆盖。目前，星链已经发射了约1900颗卫星，预计到2025年将达到4.2万颗。



对于用户来说，星链提供了高速、低延迟的网络接入服务，能够满足各种应用场景的需求。同时，星链还支持多终端设备接入，包括智能手机、平板电脑、笔记本电脑等。此外，星链还提供了一系列的增值服务，如视频点播、游戏加速等。

据了解，星链的服务价格相对较低，每月只需支付99美元即可享受高速、低延迟的网络接入服务。这对于那些生活在偏远地区或无法获得传统电信运营商服务的用户来说，无疑是一个福音。

RECOMMENDED	\$10	\$15	\$20	\$30	\$40	\$50	\$70	\$100
Example	Launches up to 100 devices	Launches up to 150 devices	Launches up to 200 devices	Launches up to 300 devices	Launches up to 400 devices	Launches up to 500 devices	Launches up to 700 devices	Launches up to 1000 devices

不过，也有一些人对星链的安全性提出了质疑。他们认为，星链可能会成为黑客攻击的目标，从而威胁用户的隐私和安全。对此，马斯克表示，星链采用了多种安全措施，包括加密算法、多重身份验证等，以确保用户的数据安全。

总的来说，星链是一项非常有前景的技术，它有望为全球用户提供高速、低延迟的网络接入服务。随着技术的不断发展和完善，相信星链将会为人类社会带来更多的便利和改变。



Describe this image?



The image depicts a young man and a young woman dressed in school uniforms walking down a staircase in a city setting. They appear to be enjoying their time together, with the man leading the way.

Which movie does this image come from?

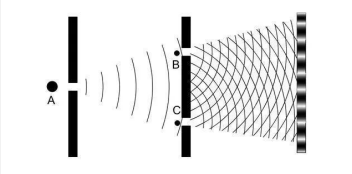


This image comes from the anime movie "Your Name."

Describe the story of this movie.



"Your Name" is a 2016 Japanese animated romantic fantasy film directed by Makoto Shinkai. The movie follows the story of a high school boy named Taki and a high school girl named Mitsuha, who find themselves mysteriously connected to each other in their dreams.



Describe this image.



The image depicts a diagram of a wave passing through a double slit experiment. There are two slits, A and B, and a single particle, represented by a black dot, is passing through one of them. The wave pattern created by the particle is shown on the left side of the diagram, while the double slit is located on the right side.

Who discovered it?



The double slit experiment was discovered by Thomas Young in 1801.



What is the funny thing in this image?



The funny thing in this image is that a car has been covered in snow, giving it the appearance of having a face. Specifically, the car has a nose, eyes, and a mouth, making it look like a snowman. This is a creative and humorous way of transforming a car into a snowman, adding a touch of whimsy to the scene.

What is the snowman's mood?



The snowman's mood appears to be happy or playful, as it has a smile on its face.



Describe this image in detail.



The image depicts a cartoonish depiction of a man's finger with a gun drawn on it. The gun is pointed directly at the man's face, creating a tense and threatening atmosphere. The man's face is also drawn on the finger, with a sad expression on his face.

Will the finger get hurt?



No, the finger will not get hurt.



能简单介绍一下这张图上的内容吗？



这幅油画描绘了一辆红色老爷车停在一座城市街道上，车旁有一棵高大的枫树。整幅画面呈现出一种宁静的氛围，似乎在讲述一段温馨的回忆。

从美学的角度分析下这副油画，聊一聊其颜色搭配、构图、光影上的特点。



这幅油画在颜色搭配上非常和谐，红色老爷车和枫树的颜色相得益彰，整个画面呈现出一种温馨、怀旧的氛围。构图上，老爷车占据了画面的主要部分，而枫树则作为背景，衬托出老爷车的风采。在光影方面，这幅油画运用了柔和的光线，使得整幅画面呈现出一种宁静、温馨的氛围。老爷车和枫树在阳光的照射下，显得更加迷人。

这种老爷车在什么时候比较流行？



这种老爷车在20世纪30年代至40年代非常流行，当时被称为“老爷车”或“老式车”。这种车型的特点是车身修长、线条流畅，通常采用V8发动机，动力强劲，适合长途驾驶。它们在美国、欧洲和澳大利亚等地非常受欢迎，成为了那个时代的一种标志性



请你描述一下这张图片



图片描绘了一个蓝色背景，上面有一只卡通时钟，钟面上显示着数字。时钟周围有一些星星和云朵，给整个画面增添了梦幻的氛围。



请你再看这张图片，它描绘了什么呢？



这张图片描绘了一个卡通女孩，她的头发是蓝色的，眼睛周围有星星和云朵，看起来非常梦幻。她的面部表情似乎有些悲伤，可能正在哭泣。

两张图片之间有相似之处吗？比如风格、背景上



两张图片在风格和背景上都有相似之处，都采用了卡通、梦幻的风格，背景都有星星和云朵的元素。



图中是什么？



麻将桌和麻将



图中的麻将牌们构成了什么番型？



图中的麻将牌们构成了“九莲宝灯”的番型

接下来，我抓到一张么鸡，请问我能胡牌吗？

是的，你抓到一张么鸡，可以胡牌。